Water Air Soil Pollut (2018) 229: 125
https://doi.org/10.1007/s11270-018-3778-1

Ciprofloxacin Adsorption on ZnO Supported on SBA-15

Watson R. D. N. Sousa · Antônio R. Oliveira · João F. Cruz Filho · Taisa C. M. Dantas · Anne G. D. Santos · Vínicius P. S. Caldeira · Geraldo E. Luz Jr

Received: 11 October 2017 / Accepted: 9 March 2018 / Published online: 22 March 2018

Abstract Most drugs are synthesized by human medicine both for the treatment of men and animals and are also produced to maintain their physical and chemical properties for a time sufficient to serve a therapeutic purpose in treatments of some kind of illness. Ciprofloxacin is an antibiotic synthetically obtained in 1987 and belongs to the family of fluoroquinolones and is currently prescribed in certain treatments. This work was developed with the objective of evaluating the adsorption of the ciprofloxacin antibiotic in solution on zinc oxide (ZnO) supported on SBA-15-type mesoporous silica. The results showed that the post-synthesis method is effective in impregnating zinc oxide in SBA-15 and its structure has not been damaged and has not lost its organization in the hexagonal 2D planes. The ZnO-SBA-15 (10%) sample adsorbed 69.10% of ciprofloxacin (25 mg/L) in 180 min. Freundlich adsorption model was observed with the correlation factor of R^2 = 0.9999, for the adsorbent ZnO-SBA-15 (10%), which showed the best sample. The kinetics was classified as pseudo-second order, as well as the thermodynamic parameters were determined, showing that the process has a spontaneous nature and a value of $\Delta H° = 4.677$ kJ/mol, evidencing that the process has the nature of physiosorption.

Keywords Zinc oxide · SBA-15 · Adsorption · Ciprofloxacin

W. R. D. N. Sousa · T. C. M. Dantas · G. E. Luz Jr,
PPGQ-DQ, Universidade Federal do Piauí –UFPI, Teresina, Piauí 64049-550, Brazil

A. R. Oliveira · J. F. Cruz Filho · T. C. M. Dantas · G. E. Luz Jr, (✉)
PPGQ-GERATEC-DQ, Universidade Estadual do Piauí, Rua: João Cabral, N. 2231, P.O. Box 381, Teresina, Piauí 64002-150, Brazil
e-mail: geraldoeduardo@gmail.com

A. G. D. Santos · V. P. S. Caldeira
PPGQ-DQ, Universidade do Estado do Rio Grande do Norte, Rua Professor Antônio Campos, s/n, BR 110, km 48, Mossoró, Rio Grande do Norte 59600-000, Brazil

1 Introduction

Medications, in general, are synthesized to maintain their physical and chemical properties for a time sufficient to serve a therapeutic purpose for some form of disease (Bila and Dezotti 2003). When administered, they can be partially metabolized and excreted in the urine and feces and, as a consequence, can enter sewage treatment plants, where traditional effluent treatment is inefficient to degrade them, thus contaminating those water resources (di Bernardo and Dantas 2005; Kolpin et al. 2002). Thus, the increased concentration of some residual drugs may cause environmental and public health impacts (Jorgensen and Halling-Sorensen 2000; Doorslaer et al. 2014). Drugs that do not undergo an effective degradation process prior to their entry with effluents into rivers and lakes generate aquatic toxicity, genotoxicity, alteration of the reproductive cycle of aquatic species, and endocrine disorders (Kümmerer et al. 2000). Among the drugs, antibiotics have the most

damaging consequences, where ciprofloxacin is one example of antibiotics. These are more active in infections against gram-negative bacteria and widely used in treatments of various types of infections, such as: urinary, respiratory, gastrointestinal, cutaneous, orthopedic, and articular (Mierzwa and Hespanhol 2005). However, a major problem is the difficult removal of these when they are released into the environment (Melo et al. 2009; Prieto et al. 2011).

Some studies investigate the removal using the adsorption method because it presents some advantages like cost-benefit, flexibility, simple design, easy operation, insensitivity to toxic pollutants, and the possibility of being reused (Klavarioti et al. 2009). Adsorbents such as the carbon materials (Ji et al. 2011; Li et al. 2014), metal oxide (Ji et al. 2013), polymers (Tan et al. 2013), and zeolites (Blasioli et al. 2014; Braschi et al. 2010) were previously studied and presented limitations as limited pore sizes, since the antibiotic molecules shown are in the nanometer range, or did not show adequate functionality for the adsorption of antibiotics, since they have complex molecular formulas and different functional groups. Developing of new adsorbents and of internal adsorption mechanisms are of great interest in the research of adsorption antibiotics (Gao et al. 2015).

Previous works reported the release of drugs using drugs similar to ciprofloxacin in different structures based on functionalized silica. García-Muñoz et al. studied the influence of textural structures and properties of these materials on the controlled release of methylprednisolone hemisuccinate, where it was observed that the structures with better properties obtained higher adsorption of the drug (García-Muñoz et al. 2014). The literature reports the functionalization of structures using different functional groups and the results showed that for the functionalized structure with the higher amine content organosilane, the amounts of drugs adsorption were higher, in relation to non-functionalized samples (Ortiz-Bustos et al. 2017; Martín et al. 2018). Drug release rates in mesoporous silica materials are strongly influenced by the adsorption behavior of the species when they are close to the functional groups on the surface, which are measured by molecular interactions at specific sites (Morales et al. 2016).

We can also cite some metal oxides as good adsorbents (Pelaez et al. 2012; Danwittayakul et al. 2015), among which titanium dioxide (TiO_2) and zinc oxide (ZnO) are widely used (Etacheri et al. 2015; Chang et al. 2016). This is because they exhibit a good stability in aqueous media, low cost, as well as environmentally favorable features (Akyol and Bayramoğlu 2005). Researchers reported impregnation of ZnO supported on silica structures, being the mesoporous silica structure. Because these materials have relatively large pore sizes (2–30 nm), they allow drugs with larger structures to access the mesoporous inner surfaces. In addition, both the internal mesochannel surfaces and external particle surfaces of mesoporous silicas can be functionalized with a variety of chemical structures that assist in a greater interaction with the pharmaceuticals and thus influence the adsorption and release properties of these species (Calvillo et al. 2008; Izquierdo-Barba et al. 2009; Gignone et al. 2015). Within the mesoporous silicas found in the literature, the SBA-15 becomes an excellent option, because they present good stability, as well as surface area and diameter of excellent pores (Babu et al. 2012). This combination showed the ability of the material as an adsorbent aiding in the removal in pollutants found in the aquatic environment (Popova et al. 2016).

This work was carried out with the purpose of studying the adsorption process of the antibiotic ciprofloxacin over ZnO supported on SBA-15 molecular sieve.

2 Experimental

2.1 Reagents

Zinc Acetate (Aldrich); potassium hydroxide (KCl, Vetec); isopropyl alcohol (Dynamic, 95%); 2-aminoethanol (MEA) (Aldrich); tetraethyl orthosilicate (TEOS, Aldrich, 98%); pluronic P123 (Aldrich); hydrochloric acid (HCl, Vetec, 37%); deionized water; ethyl alcohol (Dynamic, 95%); and 10^{-4} M ciprofloxacin solution (Aldrich, 98.9%) were used in the study.

2.2 Methods

2.2.1 Synthesis of ZnO Nanoparticles

First, 8.23 g of zinc acetate ($Zn(Ac)_2$) in 15 mL of isopropyl alcohol was added. Under this mixture, 2.3 mL MEA with 15 mL of isopropyl alcohol was added. After preparation, all solutions were mixed slowly. The final solution was then oven dried at 100 °C for 2 h and calcined for 3 h at 600 °C with an air flow rate of 100 mL/min.

2.2.2 Synthesis of SBA-15

A typical synthesis method to obtain pure SBA-15 by the hydrothermal method is described with molar ratios: 1 TEOS:0.015 P123:2.75 HCl:166.0 H_2O. Initially the pluronic P123 was dissolved in deionized water and HCl. That mixture was maintained at 40 °C for 24 h under constant stirring. The formed gel was transferred to a stainless autoclave, which was sealed in a hydrothermal system at 100 °C for 48 h. The obtained sample was washed with 50 mL of ethyl alcohol several times, vacuum filtered, and calcined at 600 °C for 4 h under refluxing air to decompose of the template (Luz Jr et al. 2010).

2.2.3 Functionalization of the SBA-15 with ZnO

The functionalization process was performed by the post-synthesis method with the addition of 0.5 g of SBA-15 in 25 mL of water, and the mixture received the nomenclature of (S1). A dispersion with the required mass of the ZnO nanocrystals was also prepared to achieve the proportion of each of the adsorbents (5, 10, and 20%) which received the (S2) nomenclature. The solutions (S1) and (S2) were mixed and subjected to constant stirring at a temperature of 80 °C until all of the liquid had evaporated. The resulting solid was collected and dried in the oven at 100 °C for 2 h and then calcined at 600 °C for 5 h with airflow rate of 100 mL/min. The same method synthesized the other samples, making the changes in the mass of the zinc oxide nanocrystals according to the mass percentage of the adsorbent.

2.3 Characterization of the Samples

For identifying the spatial arrangements of the samples, x-ray diffraction was performed in the 2θ bands of 0.5–5° and 10–80°, in low and medium angle in the Shimadzu equipment, model XRD 6000, with radiation source of CuKα ($\lambda = 0.15406$ nm), nickel filter, operating at 30 kV and 30 mA at 0.5°/min speed. The textural properties and adsorption isotherms, as well as the specific area investigation, were obtained by the Brunauer-Emmett-Teller (BET) method, using the Micromeritics ASAP-2020 equipment, with a relative pressure range (P/P_0) of 0.01 to 0.99 at the temperature of the liquid nitrogen (77 K). The micropore volume (Vmic) and area (Smic) were determined by applying the *t* plot equation to the N_2 adsorption isotherms. The software micromeritics was used to generate the non-linear density functional theory (NLDFT) pore size distribution (PSD) curves from the N_2 adsorption isotherms using adsorption branch and the kernel "N_2, 77K, Cylindrical Pores in an Oxide Surface" of the mentioned software. To determine the x-ray intensities and the density of the active sites of the adsorbents of the samples, FRX was performed using a ZnO-SBA-15 pellet in the different mass proportions (5, 10, 20%), using the Rigaku RIX 3100 equipment. The absorbance spectra of the solutions were obtained on the Shimadzu spectrophotometer, model UV-2600 in the range between 200 and 800 nm.

2.4 Adsorption Test

Adsorption was performed using the following procedure: 40 mg of the adsorbent, previously activated at 300 °C for 180 min, were dispersed in 100 mL of ciprofloxacin solution (10^{-4} mol/L). The suspension was kept under continuous agitation (without light) for 180 min at 25 °C. During that process, at certain time intervals, a 3-mL aliquot was withdrawn and the samples were centrifuged at 100 rpm using an IKA® mini G instrument for 2 min for UV-Vis analysis with 200–800 nm scanning. The process was repeated for the other adsorbents. A calibration curve was made to determine the concentration of the drug as a function of adsorption and the wavelength analyzed was 273 nm, which is the most intense band of ciprofloxacin.

The adsorbent capacity of the adsorbent, q_e (mg/g), was calculated according to Eq. (1) (Peng et al. 2016a, b).

$$q_e = (Ci - Cf).\frac{V}{M} \quad (1)$$

where q_e is the adsorbed amount (mg/g), V is the volume of the solution, and M is the adsorbent mass.

The kinetic study for the adsorption of ciprofloxacin was carried out in a batch process. An amount of 100 mL of 2.5, 5, 15, and 25 mg/L concentrations of ciprofloxacin solution were placed in contact with 40 mg of the adsorbents at a temperature of 25 ± 1 °C, with the time varying from 0 to 180 min, and the saturation equilibrium was reached in the first 60 min of the test. After each period, the supernatant was separated from the adsorbent by centrifugation (at 100 rpm for 2 min). The concentration was determined by spectrophotometry in the UV-Vis region using the equation obtained by the calibration curve previously done before

the tests. The results of the kinetics were adjusted to three kinetic models: pseudo-first order, pseudo-second order, and intra-particle diffusion (Ho and McKay 1998, 1999).

2.5 Adsorption Isotherms

The adsorption isotherms were performed by placing 40 mg of adsorbent in contact with 100 mL of ciprofloxacin solution in concentrations of 2.5 to 25 mg/L. The system was placed under stirring at 25 °C (298.15 K). After stirring, the supernatants were separated from the adsorbent by centrifugation (at 100 rpm for 2 min). The adsorbed amount was determined by spectrophotometry in the UV-Vis region (Eq. 1).

The models of Langmuir (Eq. 2) (Langmuir 1916), Freundlich (Eq. 3), and Temkin (Eq. 4) (Gessner and Hasan 1987).

$$\frac{C_e}{q_e} = \frac{1}{q^b_{\max}} + \frac{C_e}{q_{\max}} \tag{2}$$

$$\log q_e = \frac{1}{n}\log C_e + \log K_f \tag{3}$$

$$q_e = \frac{1}{n_T}\ln K_T + \frac{1}{n_T}\ln C_e \tag{4}$$

2.6 Adsorption Test with Temperature Variation

The maximum adsorbed amount per 180 min of the adsorbent was analyzed. In this study, 40 mg of the ZnO-SBA-15 adsorbent (10%) was added to 100 mL of ciprofloxacin solution of 10 mg/L and stirred for 180 min at 25 ± 1 °C, 35 ± 1 °C, and 45 ± 1 °C. At the end of the estimated time for each aliquot, the material was centrifuged at 100 rpm for 2 min and the supernatant was quantified by UV-Vis spectrophotometry.

The thermodynamic parameters $\Delta G°$ (Gibbs free energy), $\Delta H°$ (enthalpy), and $\Delta S°$ (entropy) were obtained for the adsorption processes at three different temperatures, 25, 35, and 45 °C (298.15, 308.15, and 318.15 K), using Eqs. 5 and 6:

$$\log K_e = \frac{\Delta S^\circ}{2303R} - \frac{\Delta H^\circ}{2303RT} \tag{5}$$

$$\Delta G^\circ = \Delta H^\circ - T\Delta S^\circ \tag{6}$$

where R is the gas constant (J/mol K), T is the temperature (K), and K_e is the equilibrium constant at temperature T, obtained by the Freundlich model (Gessner and Hasan 1987; Li et al. 2014).

2.7 Adsorption Test with pH Variation

The adsorption sweep of the pH values was performed with pH adjustment (in the values: 2, 5, 6, 7, 8, 9, and 12) of ciprofloxacin concentration of 10 mg/L. The pH adjustment was performed using 0.5 mol/L solutions of HCl and NaOH. Subsequently, about 100 mL of solution of each pH was added to about 40 mg of the adsorbent and placed under continuous stirring at a temperature of 25 ± 1 °C for 60 min, time required to reach equilibrium. After the shaking time was over, the samples were centrifuged at 100 rpm for 2 min and quantified by UV spectrometry.

3 Results and Discussion

3.1 X-ray Diffraction and N_2 Adsorption/Desorption

X-ray patterns in low angle, shown in Fig. 1, demonstrated that all samples show five diffraction peaks indexed to planes (100), (110), (200), (210), and (300), which are characteristic of two-dimensional mesoporous materials with P6mm symmetry, like to SBA-15 molecular sieve (Zhao et al. 1998; Sanz-Pérez et al. 2017). This fact indicates that the SBA-15 hexagonal mesoporous structure was sustained after the ZnO incorporation (Zhang et al. 2000). However, with the ZnO incorporation on the SBA-15, there was a reduction in diffraction peaks intensity, indicating the impregnation promoted the increase in mesoporous arrangement (Taghavimoghaddam et al. 2012; Sareen et al. 2015). On the other hand, for the ZnO-SBA-15 sample (10%), the effect of the impregnated amount did not significantly change the order of SBA-15 when compared to the other two impregnated samples. When observed, the diffraction peaks related to the plane (100), it is

observed a shift to higher 2θ values, which can indicate that there was a decrease of the mesoporous parameter due to ZnO insertion on SBA-15 structure (Jiang et al. 2006).

The x-ray diffraction in a wide angle of the ZnO nanocrystals employed in this research, in which all Bragg diffraction peaks are shown in Fig. 2. All Bragg diffraction peaks are typical of hexagonal zinc oxide crystals (JCPDS: 36-1451) (Chang et al. 2016). The Sheer equation determined the size of the ZnO nanoparticles, which have an average size of 39.4 nm. The results show that the synthesized ZnO nanocrystals have a hexagonal and monophasic wurtzite structure (Mayrinck et al. 2014). N_2 adsorption/desorption isotherms of all solid samples are shown in Fig. 3.

The sample of ZnO nanocrystals shown above has type-III isotherm and H3 type hysteresis, which is characteristic of nonporous with the presence of adsorbed volume related to interstitial or interparticle spaces (Carraro et al. 2014; IUPAC 2015). As the nanoparticles of ZnO are not porous, the formation of interstices between the nanoparticles of ZnO can explain the phenomenon, the material presents pore volume corroborating with the values of volumes for materials found in the literature and that present the same characteristics of these nanoparticles (Lv et al. 2011; Al-Kahlout 2014).

The samples of SBA-15 incorporated with different percentages of ZnO (Fig. 4) have a type-IV (a) isotherm with type-HI hysteresis loop (Carraro et al. 2014; IUPAC 2015), which is characteristic of uniform mesoporous materials and cylindrical pore systems, as expected when one has a molecular sieve of the SBA-15 type (Moosavi et al. 2012).

The textural properties of the samples were obtained from nitrogen adsorption/desorption isotherms, as well as by the x-ray diffraction results, and are shown in Table 1.

In the surface area data, calculated by the BET method, shown in Table 1, it is observed that a surface area decreases when the incorporated oxide content increases, which can mean that the oxide is incorporated on SBA-15 external surface (Bhuyan et al. 2018).

In addition, it is observed in Table 1 that mesoporous parameter (a_0) is smaller in impregnated samples than SBA-15 sample, as beforehand indicated by XRD patterns (Fig. 1). This fact may be associated to decrease in average pore diameter (Dp) or in wall thickness (Mihai et al. 2010). However, until analyzing Table 1, it can see that impregnated samples have a higher average pore diameter in comparison to that of SBA-15 sample. This apparent contradiction can be explained by the higher Dp of ZnO (18.16 nm) than that of SBA-15 (5.89 nm). Thereby, the ZnO incorporation on SBA-15 surface promotes an increase in the mean of pore diameter. This explanation is corroborated by average pore diameter increasing with ZnO content increase in impregnated samples.

3.2 Adsorption Result

Table 2 shows the q_e results, as well as the adsorption and kinetics study for ZnO, SBA-15, ZnO-SBA-15 (5%), ZnO-SBA-15 (10%), and ZnO-SBA-15 (20%):

From Table 2, it can be observed that the values of q_e are proportional to the incorporated amount of ZnO in the SBA-15, and that the effect of the incorporation improves the adsorption, since, when comparing the mass of pure ZnO to the one of the adsorbent ZnO-SBA-15 (20%), which is 20% of the pure, the adsorption value of ciprofloxacin is very close, showing that the process becomes more effective with the incorporation of ZnO.

Figure 4 shows the adsorption of ciprofloxacin in the sample of ZnO-SBA-15 (10%) at 25 °C (Table 3). According to the results shown in Fig. 4, it is possible to observe that the adsorption equilibrium was reached with 60 min of test in all the samples, regardless of the ZnO percentage of the sample, and that the adsorbed amount is proportional to the amount of ZnO impregnated in SBA-15.

The Freundlich model describes a non-ideal adsorption on heterogeneous surfaces with multiple layers of adsorption. That model assumes that the strongest binding sites are occupied first and that binding strength decreases with increasing site occupancy degree (Gessner and Hasan 1987; Peng et al. 2016a). In all cases, the R^2 values of Freundlich were very close to 1, showing it is the model that best suits the case. When the values of $n > 1$, there is a strong indication of the presence of highly energetic sites and the greater that difference between n and 1, the greater the distribution of that binding energy on the surface of the adsorbent. Those values can also suggest the occurrence of cooperative adsorption, in which they involve strong interactions between the molecules of the adsorbate itself, values of n between $1 < n < 10$ indicate favorable adsorption (Desta 2013; Jalil et al. 2015; Danalioğlu et al. 2017).

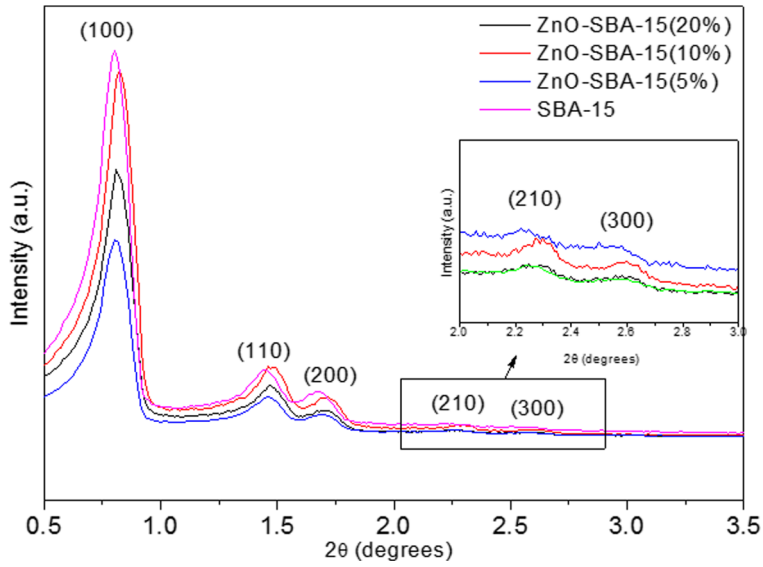

Fig. 1 XRD patterns of SBA-15, ZnO-SBA-15 (5%), ZnO-SBA-15 (10%), and ZnO-SBA-15 (20%) samples in low angle

It is also possible to observe that, for the ZnO and SBA-15 samples, the value of $n < 1$ shows an unfavorable adsorption for the pure samples. Nevertheless, in the samples where impregnation occurred, an increased value of n occurs, showing that the impregnation improves the adsorption of ciprofloxacin in the adsorbents. There is also a decreased ZnO-SBA-15 (20%) sample, which may be because the micropores are blocked in that sample, as shown in Table 1 of textural properties. The sample with the highest q_{max} is ZnO-SBA-15 (10%), with 446 mg/g, and there is a reduced value of the equilibrium constant and of n, with an increased percentage of zinc oxide incorporation in SBA-15.

From the correlation factor (R^2) values, it was possible to determine that the model that best suits that adsorption is of pseudo-second order, because the correlation values approach to 1. That adsorption mechanism shows that the reaction on the surface of the adsorbent is the step that controls the adsorption rate. The nature of the sorption process depends on the physical or chemical characteristics of the adsorbent system and on the conditions of the system (Peng et al. 2015,

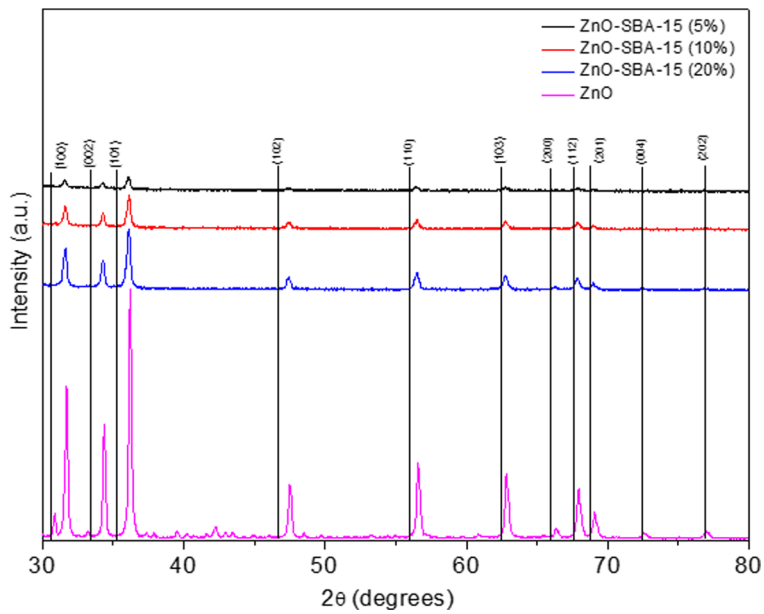

Fig. 2 XRD patterns of ZnO-SBA-15 (5%), ZnO-SBA-15 (10%), and ZnO-SBA-15 (20%) samples in wide angle

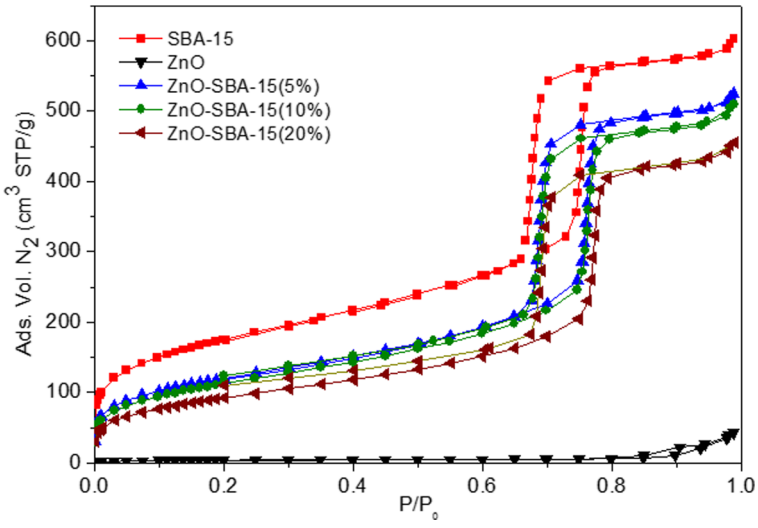

Fig. 3 N_2 adsorption/desorption isotherms of SBA-15, ZnO, ZnO-SBA-15 (5%), ZnO-SBA-15 (10%), and ZnO-SBA-15 (20%) samples

2016a). The second-order model suggests that the adsorption process of ciprofloxacin is due to the chemisorption of that material with the adsorbent, and the ZnO-SBA-15 (10%) adsorbent has the highest correlation factor among all, $R^2 = 0.9999$ (Azizian 2004; Yan et al. 2017).

That sample also has a higher velocity constant $K_2 = 0.01136$, which shows us that the adsorption velocity for that sample is the largest among the others (Peng et al. 2016a). Another relevant fact to the study is that the q_e values obtained in Table 2 are in tune with the theoretical q_e results obtained by the pseudo-second-order model; all values are very close, which shows that the model followed by the pseudo-second order is the one closest to the adsorption of ciprofloxacin in the samples Table 4 summarizes all models.

3.3 Influence of pH

Figure 5 shows the relationship between the amounts of ciprofloxacin in the ZnO-SBA-15 (10%) sample as a function of the pH of the medium. The increasing sequence of the adsorption capacity, in which increasing the hydrophobicity of mesoporous silica results in the best adsorptive property of the most hydrophilic adsorbent (Gao et al. 2015). The adsorption is proportional to

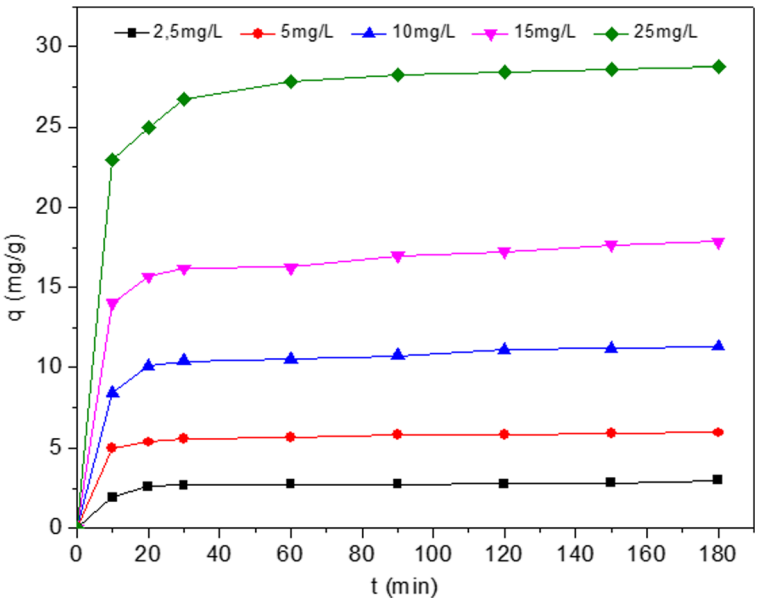

Fig. 4 Ciprofloxacin adsorption on ZnO-SBA-15 (10%)

Table 1 Textural properties of the samples determined from the nitrogen adsorption/desorption isotherms at 77 K, applying the BET, *t* plot, and NLDFT models

Samples	S_{BET}[a] (m^2/g)	S_{MIC}[b] (m^2/g)	V_{MIC}[b] (cm^3/g)	V_{MES}[c] (cm^3/g)	Dp[c] (nm)	a_0[e] (nm)
ZnO oxide	< 20	–	–	0.06[d]	–	–
SBA-15	633	87	0.03	0.85	10.6	11.5
SBA-15-ZnO 5%	436	41	0.01	0.73	11.2	11.4
SBA-15-ZnO 10%	411	13	0.00	0.69	11.7	11.1
SBA-15-ZnO 20%	337	02	0.00	0.63	11.8	11.3

[a] BET method in 0.05 to 0.2 range

[b] *t* plot method by Harkins and Jura equation

[c] Non-local density functional theory (NLDFT) method in cylindrical pores

[d] The data corresponds to total volume

[e] $a_0 = 2d(100)/\sqrt{3}$

Table 2 q_e value of the samples of ZnO, SBA-15, ZnO-SBA-15 (5%), ZnO-SBA-15 (10%), and ZnO-SBA-15 (20%)

Samples	q_e (mg/g)				
	2.5 mg/L	5 mg/L	10 mg/L	15 mg/L	25 mg/L
SBA-15	2.23	4.84	5.28	5.47	13.04
ZnO	1.89	1.98	6.11	17.43	32.58
ZnO-SBA-15 (5%)	2.61	5.44	8.62	14.02	19.89
ZnO-SBA-15 (10%)	2.98	5.95	11.33	17.84	28.78
ZnO-SBA-15 (20%)	2.63	6.22	6.32	23.24	32.28

the electrostatic interaction between the adsorbent and the adsorbate. The pH of the aqueous solution is an important parameter for controlling the adsorption process. In a low pH condition, the destruction of the zinc oxide structure occurs, being converted to Zn^{2+} ions, which inhibits the interaction between the participants, reducing the adsorption. It is observed that at values of pH < 4 and pH > 8, the sorption capacity is very low (Ghasemi and Azizi 2017). At the natural pH (near the isoelectric point of ciprofloxacin), the ciprofloxacin

Table 3 Parameters obtained with the Langmuir, Freundlich, and Temkin isotherm models for the adsorption of ciprofloxacin in samples at 25 °C (298.15 K) and saturation time of 180 min

Adsorption isotherms										
Adsorbent	Langmuir				Freundlich			Temkin		
	Q_{max} (mg/g)	B (L/mg)	R^2	R_L	n	K_f (L/g)	R^2	n_T	K_T (L/g)	R^2
SBA-15	6.139	0.383	0.9808	0.0945	0.797	0.24	0.9832	0.77	4.957	0.7097
ZnO	14.453	0.032	0.5352	0.5591	0.738	0.36	0.9097	0.08	4.1×10^{-8}	0.7769
ZnO-SBA-15 (5%)	75.586	0.015	0.6984	0.7338	1.214	1.13	0.9905	0.13	4.1×10^{-4}	0.9309
ZnO-SBA-15 (10%)	446.429	0.003	0.5196	0.9371	1.014	1.21	0.9995	0.09	5.1×10^{-6}	0.9008
ZnO-SBA-15 (20%)	134.048	0.008	0.3706	0.8261	0.895	0.99	0.9922	0.08	4.7×10^{-7}	0.9669

Table 4 Kinetic adsorption models in ciprofloxacin solution 10 mg/L

Adsorption kinetics										
Adsorbent	Pseudo-first-order			Pseudo-second-order			Inraparticle diffusion model			
	R^2	K_1 (min^{-1})	q_e (mg/g)	K_2 (g/mg/min)	q_e (mg/g)	R^2	H (mg/g/min)	K_{id} (mg/g/$min^{1/2}$)	C	R^2
SBA-15	0.8171	0.0014	0.484	9.96×10^{-3}	5.524	0.9688	0.304	0.222	2.222	0.8889
ZnO	0.2945	0.0025	1.175	8.60 × 10–4	39.541	0.8948	1.345	1.185	12.311	0.5154
ZnO-SBA-15 (5%)	0.7625	0.0009	1.159	5.86×10^{-3}	20.338	0.9974	2.424	0.585	12.270	0.8971
ZnO-SBA-15 (10%)	0.6708	0.0273	24.811	1.14×10^{-2}	29.206	0.9999	9.690	0.499	22.880	0.8011
ZnO-SBA-15 (20%)	0.6059	0.0015	1.287	2.23×10^{-3}	34.048	0.9977	2.588	1.454	14.260	0.8106

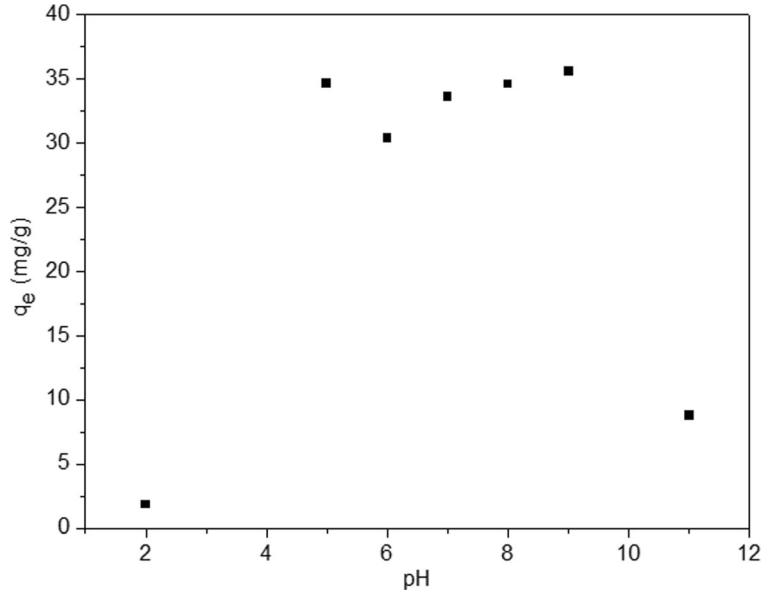

Fig. 5 Relationship between the adsorbed amounts at equilibrium (q_e) and the pH

present in the solution in zwitterionic form increases the electrostatic interaction between it and ZnO, improving the adsorption. At high pH, the ciprofloxacin present undergoes repulsive interaction between OH^- anions. For ciprofloxacin, there is protonation of the amine group at a pH below 6.1 and deprotonation of the negatively charged carboxylic group. The maximum adsorption corresponded to the zwitterionic species (Jiang et al. 2013; Ma et al. 2015; Peng et al. 2016a, b). Some studied materials reported behavior similar to that seen in the structure of ZnO (El-Kemary et al. 2010; Danalioğlu et al. 2017).

3.4 Thermodynamic Parameters

The value of Gibbs free energy ($\Delta G°$) Table 5 was calculated by the equation $\Delta G° = -RT\ln K_e$, where K_e can be the Freundlich equilibrium constant or the

Table 5 Thermodynamic parameters obtained for ciprofloxacin adsorption in samples at 25, 35, and 45 °C (298.15, 308.15, and 318.15 K)

Adsorbate	$\Delta H°$ (kJ/mol)	$\Delta S°$ (J/mol)	$\Delta G°$ at temperature (°C) (kJ/mol)		
Ciprofloxacin	4.677	29.154	298.15 K	308.15 K	318.15 K
			− 4.020	− 4.300	− 4.600

distribution constant, determined by the ratio of the amount adsorbed at equilibrium by the concentration value at equilibrium (Peng et al. 2016a). In order to determine the $\Delta G°$, the distribution constant was used, and the calculated value by the Freundlich constant is very close to the value determined by the distribution constant. Equation 10 also determined the values of $\Delta H°$ and $\Delta S°$.

The influence of temperature is an important factor in the actual application of the antibiotic removal process. Furthermore, one may observe that an increased ciprofloxacin adsorption occurs with increasing temperature, indicating that ciprofloxacin adsorption under the material is favored at higher temperatures, which shows that the process has an endothermic nature (Miao et al. 2016; Peng et al. 2015). The enthalpy variance value shows that the nature of the interaction between the active sites of the adsorbent and the adsorbate is of physiosorption (Zhang et al. 2007). The increased amount of adsorbed ciprofloxacin with increasing temperature can be attributed to the increased mobility of the molecules in solution or also the activation of some new active sites on the SBA-15, where it is seen that after the addition of metal oxide, the negative value of ΔG increased (Wang et al. 2013; Konicki et al. 2013). By the value of ΔG obtained using the K_d distribution constant, we can observe that an increased temperature also increases the spontaneity of the reaction, as shown in Table 4 (Peng et al. 2014).

4 Conclusion

The characterization results of ZnO-SBA-15 (5%), ZnO-SBA-15 (10%), and ZnO-SBA-15 (20%) adsorbents synthesized by the post-synthesis method showed that the oxide adsorption was efficient in the catalytic support and that the zinc oxide nanoparticles were efficiently synthesized by the proposed method. With the x-ray diffraction analysis, one observed that the incorporation of the zinc oxide did not damage the mesoporous structure of the SBA-15 molecular sieve. Through the N_2 adsorption and desorption analysis, one observed that there was good absorption by zinc oxide nanoparticles in the SBA-15, thus causing a decrease in the specific surface area and increase in pore volume. With UV-Vis spectroscopy, it was possible to analyze the adsorption caused by the use of the adsorbent in the ciprofloxacin solution. The Langmuir, Freundlich, and Temkin models were used to describe the isotherms, and the Freundlich model was the most adequate in comparison with the Langmuir and Temkin model, indicating the process involved in the cooperative sorption. In addition, the ZnO-SBA-15 (10%) sample had higher sorption capacity and faster adsorption rates. The kinetic model of pseudo-second order better interpreted the rates of sorption of ciprofloxacin on the samples. This study also demonstrated that neutral or zwitterionic species have significant affinity for adsorption with the material.

Funding The authors acknowledge the financial support of the Brazilian research financing CNPq (307559/2015-7; 455864/2014-4) and CAPES institutions.

References

Akyol, A., & Bayramoğlu, M. (2005). Photocatalytic degradation of remazol red F3B using ZnO catalyst. *Journal of Hazardous Materials, B124*, 241–246.

Al-Kahlout, A. (2014). Thermal treatment optimization of ZnO nanoparticles photoelectrodes for high photovoltaic performance of dye-sensitized solar cells. *Journal of the Association of Arab Universities for Basic and Applied Sciences, 17*, 66–72.

Azizian, S. (2004). Kinetic models of sorption: a theoretical analysis. *Journal of Colloid and Interface Science, 276*, 47–52.

Babu, K. S., Reddy, A. R., Sujatha, C., & Reddy, K. V. (2012). Effect of Mg doping on photoluminescence of ZnO/MCM-41 nanocomposite. *Ceramics International, 38*(7), 5949–5956.

Bhuyan, D., Saikia, M., & Saikia, L. (2018). ZnO nanoparticles embedded in SBA-15 as an efficient heterogeneous catalyst for the synthesis of dihydropyrimidinones via Biginelli condensation reaction. *Microporous and Mesoporous Materials, 256*, 39–48.

Bila, M. D., & Dezotti, M. (2003). Fármacos no meio ambiente. *Química Nova, 26*(4), 523–530.

Blasioli, S., Martucci, A., Paul, G., Gigli, L., Cossi, M., Johnston, C. T., Marchese, L., & Braschi, I. (2014). Removal of sulfamethoxazole sulfonamide antibiotic from water by high silica zeolites: a study of the involved host–guest interactions by a combined structural, spectroscopic, and computational approach. *Journal of Colloid and Interface Science, 419*, 148–159.

Braschi, I., Blasioli, S., Gigli, L., Gessa, C. E., Alberti, A., & Martucci, A. (2010). Removal of sulfonamide antibiotics from water: evidence of adsorption into an organophilic zeolite Y by its structural modifications. *Journal of Hazardous Materials, 178*(1–3), 218–225.

Calvillo, L., Celorrio, V., Moliner, R., Cabot, P. L., Esparbé, I., & Lázaro, M. J. (2008). Control of textural properties of ordered mesoporous materials. *Microporous and Mesoporous Materials, 116*, 292–298.

Carraro, P., Elias, V., Blanco, A. G., Sapag, K., Moreno, S., Oliva, M., & Eimer, G. (2014). Synthesis and multi-technique characterization of nickel loaded MCM-41 as potential hydrogen-

storage materials. *Microporous and Mesoporous Materials, 191*, 103–111.

Chang, X., Li, Z., Zhai, X., Sun, S., Gu, D., Dong, L., Yin, Y., & Zhu, Y. (2016). Efficient synthesis of sunlight-driven ZnO-based heterogeneous photocatalysts. *Materials and Design, 98*, 324–332.

Danalioğlu, S. T., Bayazit, S. S., Kerkez, Ö., Alhougbi, B. G., & Salam, M. A. (2017). Removal of ciprofloxacin from aqueous solution using humic acid- and levulinic acid- coated Fe_3O_4 nanoparticles. *Chem. Engin. Res. Design, 123*, 259–267.

Danwittayakul, S., Jaisai, M., & Dutta, J. (2015). Efficient solar photocatalytic degradation of textile wastewater using ZnO/ZTO composites. *Applied Catalysis B: Environmental, 163*, 1–8.

Desta, M. B. (2013). Batch sorption experiments: Langmuir and Freundlich isotherm studies for the adsorption of textile metal ions onto Teff straw (Eragrostis tef) agricultural waste. *Journal of Thermodynamics, 2013*, 1–6.

di Bernardo, L., & Dantas, A. D. B. (2005). *Métodos e técnicas de tratamento de água* (2° ed.). São Carlos: Rima.

Doorslaer, X. V., Dewulf, J., Langenhove, H. V., & Demeestere, K. (2014). Fluoroquinolone antibiotics: an emerging class of environmental micropollutants. *The Science of the Total Environment, 500–501*, 250–269.

El-Kemary, M., El-Shamy, H., & El-Mehasseb, I. (2010). Photocatalytic degradation of ciprofloxacin drug in water using ZnO nanoparticles. *Journal of Luminescence, 130*, 2327–2331.

Etacheri, V., Valentin, C. D., Schneider, J., Bahnemann, D., & Pillai, S. C. (2015). Visible-light activation of TiO_2 photocatalysts: advances in theory and experiments. *Journal of Photochemistry and Photobiology, 25*, 1–29.

Gao, J., Lu, Y., Zhang, X., Chen, J., Xu, S., Li, X., & Tan, F. (2015). Elucidating the electrostatic interaction of sulfonic acid functionalized SBA-15 for ciprofloxain adsorption. *Applied Surface Science, 349*(Part B), 224–229.

García-Muñoz, R. A., Morales, V., Linares, M., Gonzalez, P. E., Sanz, R., & Serrano, D. P. (2014). Influence of the structural and textural properties of ordered mesoporous materials and hierarchical zeolitic supports on the controlled release of methylprednisolone hemisuccinate. *Journal of Materials Chemistry B, 2*, 7996–8004.

Gessner, P. K., & Hasan, M. M. (1987). Freundlich and Langmuir isotherms as models for the adsorption of toxicants on activated charcoal. *Journal of Pharmaceutical Sciences, 76*(4), 319–327.

Ghasemi, S. M. S., & Azizi, A. (2017). Alkaline leaching of lead and zinc by sodium hydroxide: kinetics modelling. *Journal of Materials Research and Technology, 6*, 303–422.

Gignone, A., Piane, M. D., Corno, M., Ugliengo, P., & Onida, B. (2015). Simulation and experiment reveal a complex scenario for the adsorption of an antifungal drug in ordered mesoporous silica. *Journal of Physical Chemistry C, 119*, 13068–13079.

Ho, Y. S., & McKay, G. (1998). Sorption of dye from aqueous solution by peat. *Chemical Engineering Journal, 70*(2), 115–124.

HO, Y. S., & McKay, G. (1999). Pseudo-second order model for sorption processes. *Process Biochemistry, 34*, 451–465.

IUPAC - International Union of Pure and Applied Chemistry. (2015). Physisorption of gases, with special reference to the evaluation of surface area and pore size distribution (IUPAC Technical Report). *Pure and Applied Chemistry*, 1–19.

Izquierdo-barba, I., Sousa, E., Doadrio, J. C., Doadrio, A. L., Pariente, J. P., Martínez, A., Babonneau, F., & Vallet-Regí, M. (2009). Influence of mesoporous structure type on the controlled delivery of drugs: release of ibuprofen from MCM-48, SBA-15 and functionalized SBA-15. *Journal of Sol-Gel Science and Technology, 50*, 421–429.

Jalil, M. E. R., Baschini, M., & Sapag, K. (2015). Influence of pH and antibiotic solubility on the removal of ciprofloxacin from aqueous media using montmorillonite. *Applied Clay Science, 114*, 69–76.

Ji, L., Wan, W., Zheng, S., & Zhu, D. (2011). Adsorption of tetracycline and sulfamethoxazole on crop residue-derived ashes: implication for the relative importance of black carbon to soil sorption. *Environmental Science & Technology, 45*(13), 5580–5586.

Ji, Y.-X., Wang, F.-H., Duan, L.-C., Zhang, F., & Gong, X.-D. (2013). Effect of temperature on the adsorption of sulfanilamide onto aluminum oxide and its molecular dynamics simulations. *Applied Surface Science, 285*(Part B), 403–408.

Jiang, Q., Wu, Z. Y., Wang, Y. M., Cao, Y., Zhou, C. F., & Zhu, J. H. (2006). Fabrication of photoluminescent ZnO/SBA-15 through directly dispersing zinc nitrate into the as-prepared mesoporous silica occluded with template. *Journal of Materials Chemistry, 16*, 1536–1542.

Jiang, W.-T., Chang, P.-H., Wang, Y.-S., Tsai, Y., Jean, J.-S., Li, Z., & Krukowski, K. (2013). Removal of ciprofloxacin from water by birnessite. *Journal of Hazardous Materials, 250-251*, 362–369.

Jorgensen, S. E., & Halling-Sorensen, B. (2000). Drugs in the environment. *Chemosphere, 7*(7), 69–699.

Klavarioti, M., Mantazavinos, D., & Kassinos, D. (2009). Removal of residual pharmaceuticals from aqueous systems by advanced oxidation processes. Review article. *Environment International, 35*(2), 402–417.

Kolpin, D. W., Furlong, E. T., Meyer, M. T., Thurman, E. M., Zaugg, S. D., Barber, L. B., & Buxton, H. T. (2002). Pharmaceuticals hormones, and other organic wastewater contaminants in U.S. streams, 1999-2000: a national reconnaissance. *Environmental Science & Technology, 36*(6), 1202–1211.

Konicki, W., Cendrowski, K., Chen, X., & Mijowska, E. (2013). Application of hollow mesoporous carbon nanospheres as an high effective adsorbent for the fast removal of acid dyes from aqueous solutions. *Chemical Engineering Journal, 228*, 824–833.

Kümmerer, K., Alahmad, A., & Merschsundermann, V. (2000). Biodegradability of some antibiotics, elimination of the genotoxicity and affection of wastewater bacteria in sample test. *Chemosphere, 40*(7), 701–710.

Langmuir, I. (1916). The constitution and fundamental properties of solids and liquids. Part I. Solids. *Journal of the American Chemical Society, 38*(11), 2221–2295.

Li, H., Zhang, D., Han, X., & Xing, B. (2014). Adsorption of antibiotic ciprofloxacin on carbon nanotubes: pH dependence and thermodynamics. *Chemosphere, 95*, 150–155.

Luz Jr., G. E., Lima, S. H., Melo, A. C. R., Araujo, A. S., & Fernandes, V. J. (2010). Direct synthesis and characterization

of LaSBA-15 mesoporous molecular sieves. *Journal of Materials Science, 45*(4), 1117–1122.

Lv, K., Xiang, Q., & Yu, J. (2011). Effect of calcination temperature on morphology and photocatalytic activity of anatase TiO_2 nanosheets with exposed {001} facets. *Applied Catalysis B: Environmental, 104*, 275–281.

Ma, J., Yang, M., Yu, F., & Chen, J. (2015). Easy solid-phase synthesis of pH-insensitive heterogeneous CNTs/FeS Fenton-like catalyst for the removal of antibiotics from aqueous solution. *Journal of Colloid and Interface Science, 444*, 24–32.

Martín, A., Morales, V., Ortiz-Bustos, J., Pérez-Garnes, M., Bautista, L. F., García-Muñoz, R. A., & Sanz, R. (2018). Modelling the adsorption and controlled release of drugs from the pure and amino surface-functionalized mesoporous silica hosts. *Microporous and Mesoporous Materials, 262*, 23–34.

Mayrinck, C., Raphael, E., Ferrari, J. L., & Schiavon, M. A. (2014). Síntese, Propriedades e Aplicações de Óxido de Zinco Nanoestruturado. *Revista Virtual de Quimica, 6*(5), 1185–1204.

Melo, S. A. S., Trovó, A. G., Bautitz, I. R., & Nogueira, R. F. P. (2009). Degradação de fármacos residuais por processos oxidativos avançados. *Química Nova, 32*(1), 188–197.

Miao, M.-S., Liu, Q., Shu, L., Wang, Z., Liu, Y.-Z., & Kong, Q. (2016). Removal of cephalexin from effluent by activated carbon prepared from alligator weed: kinetics, isotherms, and thermodynamic analyses. *Process Safety and Environment Protection, 104*(part B), 481–489.

Mierzwa, J. C., & Hespanhol, I. (2005). *Água na Indústria: uso racional e reuso*. São Paulo: Oficina de Textos.

Mihai, G. D., Meynen, V., Mertens, M., Bilba, N., Cool, P., & Vansant, E. F. (2010). ZnO nanoparticles supported on mesoporous MCM-41 and SBA-15: a comparative physicochemical and photocatalytic study. *Journal of Materials Science, 45*, 5786–5794.

Moosavi, A., Sarrafi, M., Aghaei, A., Hessari, F. A., & Keyanpour-rad, M. (2012). Synthesis of mesoporous ZnO/SBA-15 composite via sonochemical route. *Micro & Nano Letters, 7*(2), 130–133.

Morales, V., Idso, M. N., Balabasquer, M., Chmelka, B., & García-Muñoz, R. A. (2016). Correlating surface-functionalization of mesoporous silica with adsorption and release of pharmaceutical guest species. *Journal of Physical Chemistry C, 120*, 16887–16898.

Ortiz-Bustos, J., Martín, A., Morales, V., Sanz, R., & García-Muñoz, R. A. (2017). Surface-functionalization of mesoporous SBA-15 silica materials for controlled release of methylprednisolone sodium hemisuccinate: influence of functionality type and strategies of incorporation. *Microporous and Mesoporous Materials, 240*, 236–245.

Pelaez, M., Nolan, N. T., Pillai, S. C., Seery, M. K., Falaras, P., Kontos, A. G., Dunlop, P. S. M., Hamilton, J. W. J., Byrne, J. A., O'shea, K., Entezari, M. H., & Dionysiou, D. D. (2012). A review on the visible light active titanium dioxide photocatalysts for environmental applications. *Applied Catalysis B: Environmental, 125*, 331–349.

Peng, X., Huang, D., Odoom-Wubah, T., Fu, D., Huang, J., & Qin, Q. (2014). Adsorption of anionic and cationic dyes on ferromagnetic ordered mesoporous carbon from aqueous solution: equilibrium, thermodynamic and kinetics. *Journal of Colloid and Interface Science, 430*, 272–282.

Peng, X., Hu, F., Lam, F. L.-Y., Wang, Y., Liu, Z., & Dai, H. (2015). Adsorption behavior and mechanisms of ciprofloxacin from aqueous solution by ordered mesoporous carbon and bamboo-based carbon. *Journal of Colloid and Interface Science, 460*, 349–360.

Peng, X., Hu, F., Huang, J., Wang, Y., Dai, H., & Li, Z. (2016a). Preparation of a graphitic ordered mesoporous carbon and its application in sorption of ciprofloxacin: kinetics, isotherm, adsorption mechanisms studies. *Microporous and Mesoporous Materials, 228*, 196–206.

Peng, X., Hu, F., Dai, H., Xiong, Q., & Xu, C. (2016b). Study of the adsorption mechanisms of ciprofloxacin antibiotics onto graphitic ordered mesoporous carbons. *Journal of the Taiwan Institute of Chemical Engineers, 65*, 196–206.

Popova, M., Trendafilova, I., Szegedi, A., Mihály, J., Németh, P., Marinova, S. G., Aleksandrov, H. A., & Vayssilov, G. N. (2016). Experimental and theoretical study of quercetin complexes formed on pure silica and Zn-modified mesoporous MCM-41 and SBA-16 materials. *Microporous and Mesoporous Materials, 228*, 256–265.

Prieto, A., Möder, M., Rodil, R., Adrian, L., & Marco-Urrea, E. (2011). Degradation of the antibiotics norfloxacin and ciprofloxacin by a white-rot fungus and identification of degradation products. *Bioresource Technology, 102*, 10987–10995.

Sanz-Pérez, E. S., Dantas, T. C. M., Arencibia, A., Calleja, G., Guedes, A. P. M. A., Araujo, A. S., & Sanz, R. (2017). Reuse and recycling of amine-functionalized silica materials for CO_2 adsorption. *Chemical Engineering Journal, 308*, 1021–1033.

Sareen, S., Mutreja, V., Singh, S., & Pal, B. (2015). Highly dispersed Au, Ag and Cu nanoparticles in mesoporous SBA-15 for highly selective catalytic reduction of nitroaromatics. *Royal Society of Chemistry, 5*, 184–190.

Taghavimoghaddam, J., Knowles, G. P., & Chaffee, A. L. (2012). Preparation and characterization of mesoporous silica supported cobalt oxide as a catalyst for the oxidation of cyclohexanol. *Journal of Molecular Catalysis A: Chemical, 358*, 79–88.

Tan, F., Suna, D., Gao, J., Zhao, Q., Wang, X., Teng, F., Quana, X., & Chen, J. (2013). Preparation of molecularly imprinted polymer nanoparticles for selective removal of fluoroquinolone antibiotics in aqueous solution. *Journal of Hazardous Materials, 244–245*, 750–757.

Wang, B., Leung, M. K. H., Lu, X. Y., & Chen, S. Y. (2013). Synthesis and photocatalytic activity of boron and fluorine codoped TiO_2 nanosheets with reactive facets. *Applied Energy, 112*(1), 1190–1197.

Yan, Z.-L., Liu, Y.-G., Tan, X.-F., liu, S.-B., Zeng, G.-M., Jiang, L.-H., Li, M.-F., Zhou, Z., Liu, S., & Cai, X.-X. (2017). Immobilization of aqueous and sediment-sorbed ciprofloxacin by stabilized Fe-Mn binary oxide nanoparticles: Influencing factors and reaction mechanisms. *Chemical Engineering Journal, 314*, 612–621.

Zhang, W.-H., Shi, J.-L., Wang, L.-Z., & Yan, D.-S. (2000). Preparation and characterization of ZnO clusters inside mesoporous silica. *Chemistry of Materials, 12*, 1408–1413.

Zhang, Y., Zhou, J. L., & Ning, B. (2007). Photodegradation of estrone and 17β-estradiol in water. *Water Research, 41*(1), 19–26.

Zhao, D., Feng, J., Huo, Q., Melosh, N., Fredickson, G. H., Chmelka, B. F., & Stucky, G. D. (1998). Triblock copolymer syntheses of mesoporous silica with periodic 50 to 300 angstrom pores. *Science, 279*, 548.